

Materials Aspects in Micro- and Nanofluidic Systems Applied to Biology

Olgica Bakajin, Eric Fountain, Keith Morton,
Stephen Y. Chou, James C. Sturm,
and Robert H. Austin

Abstract

One of the key problems in microfabrication and especially nanofabrication applied to biology is materials selection. Proper materials must have mechanical stability and the ability to hermetically bond to other surfaces, yet not bind biological molecules. They must also be wettable by water and have good optical properties. In this article, we review some of the attempts to find materials for micro- and nanofluidic systems in biological applications that satisfy these rather conflicting constraints. We discuss the materials properties that make poly(dimethylsiloxane) or non-elastomeric materials more or less suitable for particular applications in biology. We also explore the effects and the importance of surface treatments for integrating biological objects into microfabricated and nanofabricated fluidic devices.

Keywords: *biological, fluidics, nanoscale, surface chemistry.*

Introduction

Biological molecules and silicon technology have an uneasy relationship, yet each needs the other. Micro- and nanofluidic systems that have been used for DNA analysis, studies of protein folding, and cell separation offer several advantages over conventional macroscopic methods. Microfluidic systems are commonly associated with micro total analysis systems, which perform all the necessary analytical steps automatically on a single chip, with applications in biosensing and medical diagnostics or drug delivery.^{1,2} Micro- and nanotechnology, however, are also enabling unprecedented advances in the study of biological physics.³⁻⁵ We can now investigate single-molecule dynamics and perform experiments faster and with considerably lower consumption of

precious sample volumes. Microfluidic devices reduce analytical sample consumption by many orders of magnitude, which is especially important when heavily engineered molecules are used, such as proteins labeled with fluorophores for Foerster resonance energy transfer (FRET) analysis. Nanotechnology has the potential to revolutionize biology through the construction of chip-based devices that can not only detect and separate single DNA molecules by size, perform restriction mapping on single DNA molecules, and study DNA protein interactions, but also hopefully separate the rare one-in-a-million cell, analyze it, and sequence single DNA molecules. The confinement of DNA, which has a persistence length of 50 nm in double-stranded form, in

nanofluidic channels has enabled studies of DNA protein interactions on a single-molecule level.^{6,7}

Due to the reduction in the size of the structures around which the fluids flow, the Reynolds number is, however, typically much less than 1, even at velocities of 10 cm/s in microstructures, so that alternatives to turbulence must be found in order to generate three-dimensional flows to mix reagents efficiently. Reduced dimensions, on the other hand, allow samples to diffuse faster from one end to the other of the device. Brody et al.⁸ proposed hydrodynamic focusing—in which a slow-moving sample stream is sheathed in a faster-moving stream, enabling control of the width of the sample stream—as a way to reduce diffusion lengths under laminar-flow conditions, a method that has since been used for the study of protein-folding kinetics using various spectroscopic methods.^{3,4} This hydrodynamic focusing technique allowed observations of folding reaction kinetics on time scales that are orders of magnitude shorter than the conventional mixing methods, as well as the first observations of folding kinetics at the single-molecule level.⁵ The biggest challenges in the fabrication of devices for DNA and protein analysis lie in sealing the nanostructures, bonding dissimilar materials, and passivating surfaces. Surface passivation, which refers to treatments that reduce the tendency of biological molecules to bind to surfaces, becomes increasingly important as the dimensions of microfabricated structures decrease, because of the surface-to-volume ratio, which scales, of course, as the inverse of the characteristic size L of the space.

Since the interrogation of proteins and nucleic acids is done using various spectroscopic methods, it is necessary that the materials from which the observation windows on the microfabricated flow cell are made are transparent to the desired wavelengths. At the same time, it is important that the chosen materials can be micromachined into structures that allow appropriate fluid manipulations, such as the fast mixing required for measurements of protein-folding kinetics. While silicon still remains the material of choice for high-aspect-ratio feature etching, materials traditionally used in spectrograph cuvettes, such as fused silica (also called quartz or amorphous quartz) or calcium fluoride, are most desirable as the observation windows, due to their low fluorescence and high transmittance in the UV, visible, and IR ranges. This creates the challenge of bonding dissimilar materials or fabricating the structures in optical ma-

terials for which high-aspect-ratio etching is not as readily available.

Each size regime of micro/nanofabrication has its own set of problems. At the micrometer length scale, for example, there is interest in using structures to sort cells in whole blood.^{9,10} However, most materials are *not* biocompatible with cells, especially the white blood cells of the immune system that are often the target of interest. Highly charged surfaces like glass are poor candidates, because they avidly bind positively charged objects such as certain cells and biomolecules irreversibly. Also, immunologically foreign surfaces like silicon will trigger an immune response in the white cells, and they will bind strongly to an untreated surface. Even a hydrophobic surface such as silicone binds proteins, since proteins will bind to both hydrophobic and hydrophilic surfaces. As one moves into the nanofabrication area, one meets further problems: sealing of nanostructures now must be truly hermetic at the molecular level, surface properties become ever more important as the surface-to-volume ratio rises, and the pressures needed to maintain flow rates of interest rise to the 100 MPa level, requiring very strong bonds. Also, surface defects in materials become more important as sizes shrink, because these defects can act as blockages in nanodevices.

Elastomers: Promise and Problems

Whitesides and his colleagues championed the use of the elastomeric material poly(dimethylsiloxane) (PDMS) as a material for microfabrication,¹¹ and Quake and his colleagues through the company Fluidigm have done a great deal to move this technology forward.¹² PDMS has the basic formula $[\text{SiO}(\text{CH}_3)_2]_n$ and in the uncross-linked state above the glass transition is a viscoelastic liquid used in products like Silly Putty. When PDMS is cross-linked, typically using a platinum catalyst, and is above the glass-transition temperature, it becomes an elastomeric solid. For basic tubes, valves, and pumps, PDMS is a wonderful material because of its low Young's modulus E_s . Due to its composition—many chain segments that are entropically disordered—PDMS has the high deformability of rubber and hence low E_s .¹³ In many aspects of microfabrication that involve plumbing of liquids, the basic advantage of PDMS comes from its low E_s , which makes for relatively easy construction of valves and pumps.

However, this same elasticity gives rise to advantages and problems involving mechanical stability of two kinds, bending and buckling. In the case of bending sta-

bility, consider a beam of surface moment of inertia I_s and Young's modulus E_s cantilevered and under the influence of gravity (see Figure 1a). The deflection $y(x)$ is given by¹⁴

$$E_s I_s \frac{\partial^4 y}{\partial x^4} = \rho g, \tag{1}$$

where ρ is the density of the beam and g is the acceleration due to gravity. The displacement of a horizontally laid beam $y(x)$ is given by

$$y(x) = \frac{\rho g x^4}{24 E_s I_s}. \tag{2}$$

The measured E_s of PDMS is a function of the composition of the PDMS and the curing cycle, but as a rule of thumb, $E_s \sim 1$ MPa is a baseline modulus for PDMS. This can be compared to a typical material such as nylon, which has $E \sim 10^9$ Pa. The exceptionally low moduli for elastomeric solids with light cross-linking, basically 10^{-3} that of conventional plastics, are extremely important numbers to be used in design. Equation 2 is quite useful for calculating the deformations experienced by PDMS structures under forces.

A related problem but trickier to analyze is the buckling instability of an axially loaded beam. The buckling instability is due to growth of a bend in the loaded beam, and as the bend radius decreases, there is a critical radius beyond which the

axial force F decreases with decreasing radius: the beam buckles (see Figure 1b). The general equation for axial loading is

$$\frac{\partial^2 y}{\partial x^2} = -\frac{F}{E_s I_s} y. \tag{3a}$$

This equation has a stable solution only as long as

$$F < \frac{\pi E_s I_s}{L^2}, \tag{3b}$$

where L is the length of the beam under axial load. If the aspect ratio of the beam becomes too large for soft materials such as PDMS, then very small forces will buckle the beam.

This easy bending of PDMS structures can be used to good advantage as a built-in force calibration. In an example from our own work,¹⁵ a "bed of nails" made of silicone was fabricated by casting PDMS from an etched silicon wafer mold. Silicon wafers are patterned with an array of cylindrical pits. Briefly, the desired pattern is replicated in positive photoresist by photolithography. Bare parts of the wafers are then etched by the deep Si etching process down to the desired depth to obtain the negative pattern of the array. After cleaning, the wafers are silanized with a partially fluorinated trichlorosilane in vapor phase to facilitate the release of the elastomer from the wafers after curing. A liquid silicone prepolymer (PDMS Sylgard 184, Dow-Corning) is then poured over the silicon template, cured at 65°C for 12 h, and then peeled off of it. After release from the mold, the replica is oxidized and sterilized in an air plasma for 2 min. This process makes the PDMS surface hydrophilic. Figure 2 shows scanning electron microscopy (SEM) images of the bed of nails and the deformations caused by cells on the bed of nails. Using SEM observation, we have measured the dimensions of the pillars and calculated the spring constant of the posts. The deflection y of the posts as cells traversed the bed of nails could then be used to calculate, using Equation 2, the effective force that the cytoskeleton exerted on the nails. With this method, we can obtain a dynamic cartography of the developed forces with high spatial and temporal resolution.

If the bending and buckling were totally reversible, they could be viewed as a good aspect of the soft materials nature of PDMS, but there is another factor which makes extreme deformations irreversible, namely, the surface adhesion coefficient γ_s (units of J/m²) of PDMS. When a material with finite γ_s deforms and touches another

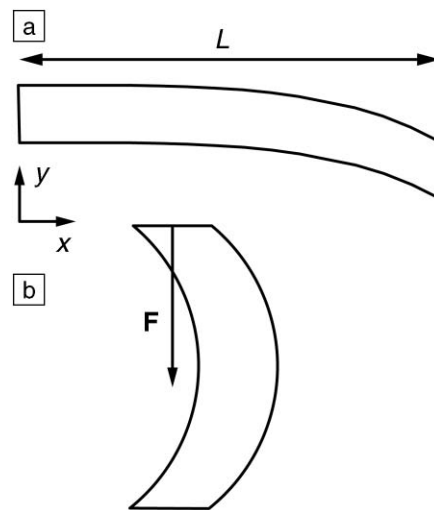


Figure 1. (a) Schematic illustration of a cantilevered beam, bent under gravitational forces. (b) An axially loaded upright beam loaded by an external force F .

surface, there are two competing interaction terms in the potential energy of the deformed material: the positive elastic strain energy U_{strain} and a negative surface interaction term U_{adhesion} . As we have

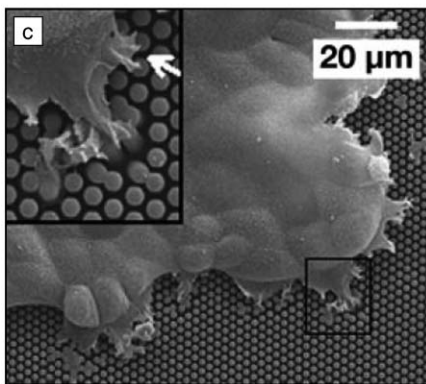
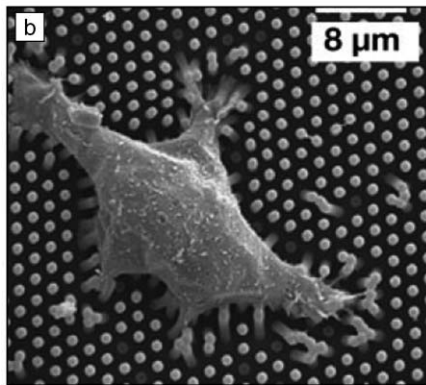
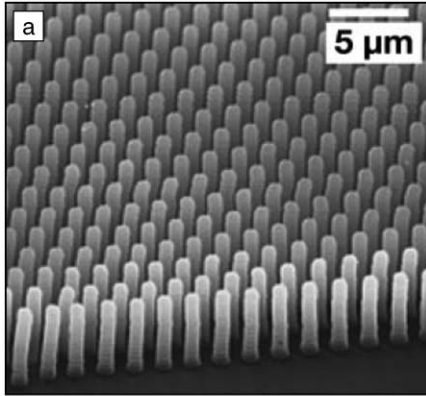


Figure 2. (a) Closely spaced microfabricated posts after poly(dimethylsiloxane) (PDMS) molding. (b) Individual cells lying on PDMS posts (1 μm in diameter and separated by 2 μm center-to-center). (c) A cell monolayer on posts 2 μm in diameter separated by 3 μm center-to-center. (c) (Inset) Magnified view (20 μm × 20 μm) of the area delineated by the black square. Cells spread only on the top of the pillar. Taken from Reference 15.

mentioned, PDMS very easily seals to surfaces. A major part of the apparently avid surface-wetting property of siloxane-based materials such as PDMS is related, strangely, to the very *small* value of its surface adhesion coefficient. Most materials, in their vacuum-cleaned state, have quite large γ_s values, typically on the order of 5 J/m²,¹⁶ while for PDMS a typical value is 0.05 J/m². The origin of the unusual and counterintuitive surface-wetting capability of PDMS, while likely connected to the partial cross-linking of the polymer chains and the hydrophobic nature of the methyl groups, is not well understood. A truly quantitative theory of γ_s is lacking, although there have been recent advances using density functional theory.¹⁷

A simple measure of both the elasticity of cross-linked PDMS and its surface-wetting ability is the detachment length l_d . We take this analysis from References 18 and 19. Qualitatively, l_d is measured by slowly moving a cantilevered length L of PDMS (or any other transparent material whose surface adhesion energy one wants to measure) an increasing distance h from another surface. The length l_c that is “wet” can be optically observed by the lack of interference fringes on the contacted region. This distance l_c will slowly decrease with increasing h until suddenly at the critical distance l_d the material will spring from the surface (see Figure 3 for an illustration of this process). The total energy U_T of a PDMS slab of thickness t , width w , and

cantilevered length L with contact length l_c is given by

$$U_T = U_{\text{strain}} + U_{\text{adhesion}} = \frac{6E_s I_s h^2}{(L - l_c)^3} - \gamma_s w l_c \quad (4)$$

where I_s is the surface moment of inertia of the beam. The actual value of l_c is determined by minimizing dU_T/dl_c . At the critical distance for detachment l_d there is no solution for l_c . This occurs at

$$l_d = \left(\frac{3E_s t^3 h^2}{2\gamma_s} \right)^{1/4} \quad (5)$$

Thus, from measurements of l_d one can extract measurements of γ_s . The measured values for γ_s for various surfaces can be found in Reference 19 and are quite sensitive to the mating surface, ranging from 0.9 N/m for PDMS on PDMS to 0.09 N/m for PDMS on SiO₂.

As we have mentioned, elastomeric materials such as PDMS display surprising adhesiveness that greatly alleviates the bonding problem in microfluidic devices. However, in some of our techniques, such as cell sorting, we make arrays of obstacles which need high aspect ratios (height h to width w) of 10:1 or higher, and then the troubles with PDMS begin. As Equation 4 makes clear, the surface adhesiveness of PDMS allows materials to stick to one another, and the soft modulus of elastomeric solids makes it easy to bend the materials. Thus, if the aspect ratios become too high and if the separation distance h between the objects becomes too small, then Equation 4 predicts that the PDMS structures if bent will stick to each other, and the bonding capabilities of PDMS become a liability rather than an asset. It is unfortunately quite easy to demonstrate this effect. Figure 4 shows an SEM image of a PDMS post structure cast from a deep-etched silicon wafer. The PDMS posts are 10 μm in diameter and 25 μm tall. One can easily see how any bending of the PDMS posts that puts them in contact with each other results in the tops adhering to each other, as we explained using Equation 2. Clearly, this is a disaster for any high-aspect-ratio post structure.

A related disaster in PDMS designs comes from using PDMS as a sealing material on etched structures where the depth h of the etch in Equation 4 is too shallow. In that case, the PDMS can deform into the area that needs to be kept open and, in combination with the high adhesion energy of elastomeric solids, can also seal the region shut. The ability of

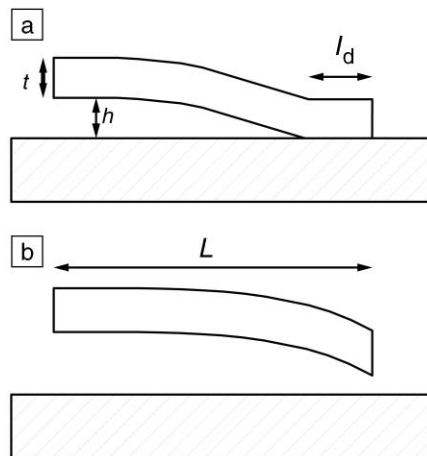


Figure 3. (a) At the point of detachment of the two surfaces, the elastic deformation energy is equal to the adhesion energy. The thickness of the beam is given by t . (b) If distance h is increased slightly beyond the critical height, the material springs from the surface.

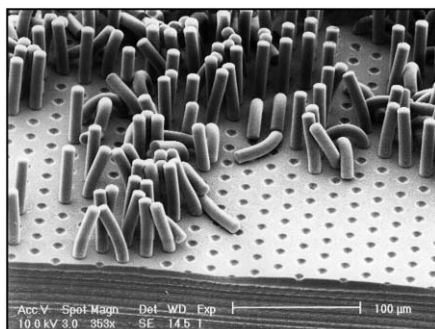


Figure 4. Scanning electron microscopy (SEM) image of an array of PDMS posts that have adhered to each other after mechanical bending, due to their surface adhesion energy.

PDMS to deform into structures is due to another materials property called surface energy, and it is to be distinguished from the surface adhesion energy γ_s discussed earlier.

We have attempted in the past, of course, to use PDMS as a gasket material to seal nanostructures; a dramatic image of a 20- μm -thick PDMS layer applied to an array of 400-nm-diameter posts etched in fused silica is shown in Figure 5. As you can see, the low modulus of PDMS and high adhesion energy makes for major problems.

Non-Elastomeric Materials

Microfluidic devices used for the study of protein and RNA folding have generally been made out of less elastic materials than PDMS, and PDMS has been used only as a sealing gasket. These applications require high-aspect-ratio micrometer-sized structures and excellent optical properties

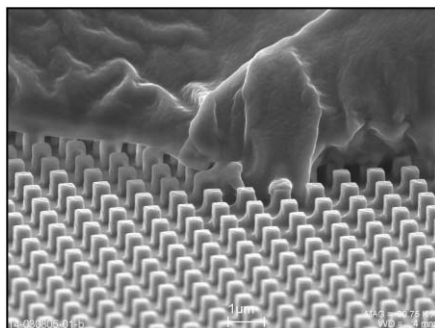


Figure 5. SEM image of 20- μm -thick PDMS layer on top of a 500-nm-deep etched array of 400-nm-diameter fused-silica posts. The PDMS has extruded itself into the interpost regions and the device is now blocked to fluid flow.

in a wide range of wavelengths. From the previous discussions, it is clear that the PDMS is less than ideal for fabrication of high-aspect-ratio structures. In addition, PDMS does not have the optical properties required for spectroscopy, and it will sustain a certain amount of damage from high-energy light (i.e., 266 nm, commonly used to probe tryptophan fluorescence).

Kauffman et al.⁴ have used an IR-transparent mixing device to study a β -sheet to α -helix transition in β -lactoglobulin protein. The channels in their device were etched in undoped silicon and sealed with calcium fluoride window-mounted using a sub-micrometer-thick layer of PDMS as a gasket. The Pollack laboratory²⁰ at Cornell University has been investigating RNA and protein folding using small-angle x-ray scattering (SAXS). The channels for these applications are through-etched in silicon, and the top and bottom are made out of PDMS.²⁰ For the measurements of microsecond protein-folding kinetics using FRET in the visible spectrum, Hertzog et al.²¹ have used mixers etched in silicon and bonded to a 170- μm -thick Pyrex glass observation window using anodic bonding. The same materials have been used for the devices with which researchers performed the first measurements of the protein-folding reaction far from equilibrium on a single-molecule level.⁵

An advantage of Pyrex glass is that it is designed for bonding to silicon, with a matching coefficient of thermal expansion and imbedded sodium ions that enable anodic bonding. Disadvantages are that it does not transmit UV light, and that creates a low fluorescent background that lowers the signal-to-noise ratio in the single-molecule measurements. Fused silica is the material of choice for many micro- and nanofluidic devices, because of its excellent optical properties.²² Unfortunately, fused silica can be difficult to bind

to other materials using thermal techniques, because of its very low coefficient of linear thermal expansion,

$$\beta = -\frac{1}{L} \left(\frac{\partial L}{\partial T} \right), \quad (6)$$

where T is temperature, compared with other materials such as silicon (fused silica has a coefficient of thermal expansion β value of $0.6 \times 10^{-6} \text{ K}^{-1}$, while Si has a β value of $3 \times 10^{-6} \text{ K}^{-1}$).

Since fused silica cannot be anodically bonded to silicon, to create devices compatible with UV spectroscopy, researchers have resorted to holding the windows over a polymer mixer structure by compressing the sandwich of window/polymer/window.²³ Alternatively, they have fabricated structures in fused silica and used fused-silica-to-fused-silica fusion bonding via reverse RCA treatment (first cleaning with RCA-2 then with RCA-1). RCA is the industry standard for removing contaminants from wafers; it is named after the company that developed the technique in 1965. Figure 6 shows an SEM image of the high-aspect-ratio (1:10) fast mixer etched in fused silica that is currently used for protein-folding studies. Using the first method,²³ cheap devices can be made, but their minimum dimensions are limited and the device sample consumption of 10 ml/min is quite high.

On the other hand, reactive ion etching of high-aspect-ratio structures in fused silica is only now becoming available and can be costly. In addition, the fusion bonding of fused silica requires two bonding steps: pre-bonding after the reverse RCA treatment and then the fusing step at 1000°C. Figure 7 shows an array device designed to fractionate objects at the 100-nm scale²⁴ which is a fused-silica-fused-silica bonded structure. These kinds of

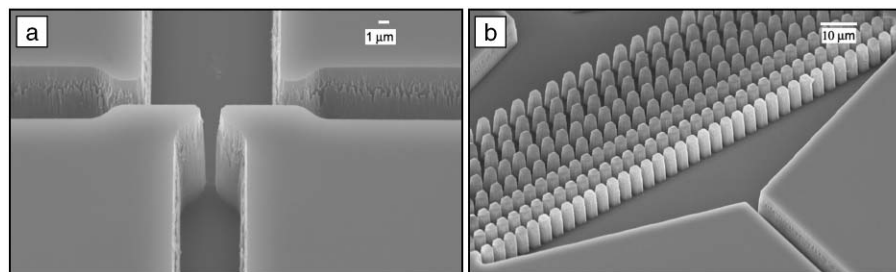


Figure 6. SEM image of a microfluidic mixer etched in fused silica that is currently being used for protein-folding measurement in one of our labs (Bakajin). (a) Mixing region; (b) image of the built-in array of posts used for on-chip filtration of solutions before they reach the mixing region.

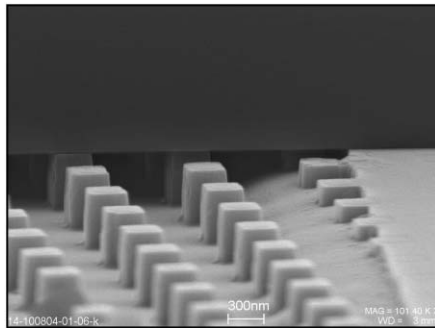


Figure 7. SEM image of a fused-silica–fused-silica bonded nanoimprinted array. The hydroxyl groups have been activated to form a hermetic seal.

bonds are hermetic at the molecular level and are suitable for nanofluidic applications.

Another alternative for microfluidic devices used for spectroscopy is the fabrication method developed by Jackman et al.,²⁵ where the channels are fabricated in SU-8 polymer and the fused-silica windows are bonded on top and bottom. This allows the spectroscopic observations to be done through pristine, unetched fused-silica windows and may have advantages for adsorption-based or circular dichroism spectroscopy where etch-induced surface roughness may interfere with the signal-to-noise ratio.

Surface Treatment: Modification of Bulk Material Properties

Most biological objects, be they proteins or cells, need to be in a saline, aqueous environment. This means that a microfabricated or nanofabricated structure has to be wetted by water. While hydrophilic surfaces like glass and fused silica wet well, they are also more prone to having biological materials adhere to them. Various methods for surface passivation are being developed in order to create non-fouling surfaces. At the nanometer scale, with extremely high surface-to-volume ratios, this is a difficult task, and the topic could be the focus of another review article. In the remainder of this article, we focus on surface treatments that change hydrophobic surfaces into hydrophilic ones, a prerequisite to introducing water into sub-micrometer-scale channels with pressure drops that are experimentally accessible.

The ability of a material to be wet by water is related to the surface tension of the fluid and the contact angle that the fluid makes with the surface of the material.²⁶ The surface tension σ (units of N/m) relates the internal pressure P inside a

sphere of liquid to the radius R of the sphere and the surface tension:¹⁶

$$P = \frac{2\sigma}{R}. \quad (7)$$

Water has a surface tension σ_w of 0.073 N/m, which is quite high compared with other liquids such as ethanol (0.023 N/m). When water comes in contact with the surface of a material, there is a competition between the self-attraction of the water molecules for each other and the attraction of the liquid for the surface of the material. This attraction modifies the effective surface tension of the liquid, and the parameter of interest is now the contact angle α between the liquid and the material. The angle is measured from the arctangent of the tangent line of the liquid at contact and the line of the surface of the material. Thus, a contact angle of 0° indicates that the liquid avidly wets the material, while a contact angle of 180° indicates complete expulsion of the liquid from the surface. Materials with low contact angles with water are called hydrophilic surfaces, while those with large contact angles are called hydrophobic surfaces.

Clean silicon (the semiconductor) and PDMS are very hydrophobic (contact angle of water on PDMS is 109° ,²⁷ on HF-cleaned silicon it is 70° ²⁸), while clean glass (SiO_2) has a contact angle of $5\text{--}25^\circ$.²⁹ The impact of these numbers comes into play when one tries to wet a microfabricated or nanofabricated structure, a capillary action problem. The pressure drop ΔP acting across the interface between a liquid of surface tension σ into a tube of radius R made of a material with contact angle α is

$$\Delta P = -\frac{2\sigma \cos(\alpha)}{R}. \quad (8)$$

A negative pressure here means that the liquid moves spontaneously into the tube and wets it in the absence of applied pressure, while a positive pressure (for $\alpha > 90^\circ$) means that the liquid must be forced in. Unfortunately for hydrophobic materials (such as PDMS), the required pressures become quite high, on the order of 1 MPa for a tube diameter of 200 nm and a contact angle of 120° . There is a related equation, called Washburn's equation, which computes the time t it takes for a liquid of viscosity η to wet a microfabricated structure with average pore size D and contact angle α in the absence of applied external pressure:

$$t = \frac{4L^2\eta}{\sigma \cos(\alpha)D}. \quad (9)$$

In order to wet microfabricated materials, and especially nanofabricated materials, the surface of the material must be pretreated with something that will lower the contact angle α of most materials and increase the surface energy γ_s that we discussed in Equations 4 and 8. The first line of offense here is to plasma-treat the surface using a glow discharge of a gas (typically O_2 , but a large range of gases can be used). There are excellent places to dive into this literature.^{30,31} The plasma discharge contains reactive, excited states of atoms and is remarkably powerful in transforming the bulk materials properties into something quite different than the bulk. One of us can remember that when he started changing the surface energy of PDMS with an O_2 plasma to make it hydrophilic, a colleague was against it because we were "ashing" the material. In fact, while it is true that plasma-surface modifications are complex, one is hardly destroying the surface. There are many manufacturers of plasma surface-modification equipment, which we invite the reader to find on the Internet.

In the case of PDMS, the fundamental problem is its contact angle α , 109° ,²⁷ which indicates that PDMS is hydrophobic, and from Equation 9, its micromachined interior will not spontaneously wet. If PDMS is treated with O_2 plasma, the oxygen radicals create negatively charged groups on the surface, and the contact angle drops to about $5\text{--}25^\circ$.²⁷ If the treated PDMS sides are put together within 1/2 h of the plasma treatment, the sealed device will wet spontaneously. This hydrophilic surface modification is not permanent. If the PDMS is kept in air after the treatment, it becomes hydrophobic, due to the movement of neutral groups to the surface. On the other hand, if PDMS is kept under water after treatment, it remains hydrophilic because the water keeps the $-\text{OH}$ groups created by the oxygen plasma at the surface. In that case, the PDMS remains hydrophilic as long as it is immersed in the water.

Another example of the power of plasma surface treatment is the improvement in the bonding of surfaces to each other. Sometimes it is desirable to permanently bond the PDMS to a surface such as glass. This is necessary if high pressures are needed, often a necessity in nanofluidic systems. In that case, the PDMS and the surface to be bonded can be plasma-treated with a combination of O_2 and H_2O gases in the vacuum chamber. The presence of the H_2O results in the creation of $-\text{OH}-$ groups at the surface of the PDMS and at the mating surface.³² Plasma surface treatment in this case enables us to

bond PDMS to a glass substrate permanently, allowing the application of high pressure.³³

Conclusions

We have briefly discussed how some common and not so common materials properties strongly influence the usefulness of a given material in micro- and nanofabricated devices. Some of the properties, such as the elasticity of the material, are obvious. Some of them, such as the surface adhesion energy, are not so obvious, nor are they well understood, but they are of critical importance. We have also discussed, however briefly, how the surface properties of the material such as the wetting contact angle can be modified, and how critical these parameters are if the goal is to bring biological objects into microfabricated and nanofabricated structures. We hope we have whetted the reader's appetite to explore this field at a depth greater than possible in this short review.

Acknowledgments

The work of O. Bakajin was performed under the auspices of the U.S. Department of Energy by the University of California's Lawrence Livermore National Laboratory under contract W-7405-Eng-48 and partially supported by funding from the Human Frontiers Science Program and the Center for Biophotonics, an NSF Science and Technology Center, managed by the University of California, Davis, under cooperative agreement PHY 0120999. The work at Princeton University was supported by grants from DARPA (MDA972-00-1-0031), NIH (HG01506), the NSF Nanobiology Technology Center (BSCECS9876771), the State of New Jersey (NJCST 99-100-082-2042-007) and U.S. Genomics. It was also performed in part at the Cornell NanoScale Science and Technology Facility (CNF), which is supported by the National Science Foundation under grant ECS-9731293, its users, Cornell University and Industrial Affiliates. We thank Abraham Stroock for many useful suggestions to the text.

References

1. S.Y.F.W. Hawkes, M.J.V. Chapela, and M. Montembault, *Combinatorial Sci.* **24** (2005) p. 712.
2. A.P. Doig, *Genetic Eng. News* **25** (2005) p. 26.
3. L. Pollack, M. Tate, N. Darnton, J.B. Knight, S.M. Gruner, W.A. Eaton, and R.H. Austin, *Proc. Natl. Acad. Sci. USA* **96** (1999) p. 10115.
4. E. Kauffmann, N.C. Darnton, R.H. Austin, C. Batt, and K. Gerwert, *Proc. Natl. Acad. Sci. USA* **98** (12) (2001) p. 6646.
5. E.A. Lipman, B. Schuler, O. Bakajin, and W.A. Eaton, *Science* **301** (2003) p. 1233.

6. Y.M. Wang, J.O. Tegenfeldt, W. Reisner, R. Riehn, X.-J. Guan, L. Guo, I. Golding, E.C. Cox, J.C. Sturm, and R.H. Austin, *Proc. Natl. Acad. Sci. USA* **102** (2005) p. 9796.
7. R. Riehn, M. Lu, Y.M. Wang, S.F. Lim, E.C. Cox, and R.H. Austin, *Proc. Natl. Acad. Sci. USA* **102** (2005) p. 10012.
8. J. P. Brody, P. Yager, R.E. Goldstein, and R.H. Austin, *Biophys. J.* **71** (1996) p. 3430.
9. J.P. Brody, Y. Han, R.H. Austin, and M. Bitsensky, *Biophys. J.* **68** (1995) p. 2224.
10. R.H. Carlson, J.P. Brody, S. Chan, C. Gabel, J. Winkleman, and R.H. Austin, *Phys. Rev. Lett.* **79** (1997) p. 2149.
11. G.M. Whitesides, E. Ostuni, S. Takayama, X.Y. Jiang, and D.E. Ingber, *Annu. Rev. Biomed. Eng.* **3** (2001) p. 335.
12. S.R. Quake and A. Scherer, *Science* **290** (2000) p. 1536.
13. M. Doi and S.F. Edwards, *The Theory of Polymer Dynamics* (Oxford University Press, Oxford, U.K., 2001).
14. J.M. Gere and S.P. Timoshenko, *Mechanics of Materials* (PWS-Kent Publishing, New York, 1984).
15. O. du Roure, A. Saez, A. Buguin, R.H. Austin, P. Chavrier, P. Siberzan, and B. Ladoux, *Proc. Natl. Acad. Sci. USA* **102** (2005) p. 2390.
16. J.A. Venables, *Introduction to Surface and Thin Film Processes* (Cambridge University Press, Cambridge, U.K., 2000).
17. A.E. Mattsson and W. Kohn, *J. Chem. Phys.* **115** (2001) p. 3441.
18. C.H. Mastrangelo and C.H. Hsu, *Proc. IEEE Solid-State Sensors and Actuators Workshop* (Hilton Head, S.C., 1992) p. 208.
19. D. Armani and C. Liu, *12th Int. Conf. on MEMS (MEMS '99)* p. 222.
20. R. Russell, I.S. Millett, M.W. Tate, L.W. Kwok, B. Nakatani, S.M. Gruner, S.G.J. Mochrie, V. Pande, S. Doniach, D. Herschlag, and L. Pollack, *Proc. Natl. Acad. Sci. USA* **99** (2002) p. 4266.
21. D.E. Hertzog, X. Michalet, M. Jager, X.X. Kong, J.G. Santiago, S. Weiss, and O. Bakajin, *Anal. Chem.* **76** (24) (2004) p. 7169.
22. W. Reisner, K.J. Morton, R. Riehn, Y.M. Wang, Z. Yu, M. Rosen, J.C. Sturm, S.Y. Chou, E. Frey, and R.H. Austin, *Phys. Rev. Lett.* **94** 196101 (2005).
23. O. Bilsel, C. Kayatekin, L.A. Wallace, and C.R. Matthews, *Rev. Sci. Instrum.* **76** (1) 014302 (2005).
24. L.R. Huang, E.C. Cox, R.H. Austin, and J.C. Sturm, *Science* **304** (2004) p. 987.
25. R.J. Jackman, T.M. Floyd, R. Ghodssi, M.A. Schmidt, and K.F. Jensen, *J. Micromech. Microeng.* **11** (3) (2001) p. 263.
26. P.-G. de Gennes, F. Brochard-Wyart, and D. Quere, *Capillarity and Wetting Phenomena: Drops, Bubbles, Pearls, Waves* (Springer, Heidelberg, 2004).
27. S. Bhattacharya, A. Datta, J.M. Berg, and S. Gangopadhyay, *J. Microelectromech. Sys.* **14** (3) (2005) p. 590.
28. Q.Y. Tong and U. Goesele, *Semiconductor Wafer Bonding* (Wiley, New York, 1999) p. 55.
29. S. Bouaidat, O. Hansen, H. Bruus, C. Berendsen, N.K. Bau-Madsen, P. Thomsen, A. Wolff, and J. Jonsmann, *Lab Chip* **5** (8) (2005) p. 827.

30. C.M. Chan, T.M. Ko, and H. Hiraoka, *Surf. Sci. Rep.* **24** (1996) p. 1.
31. C.M. Chan, *Polymer Surface Modification and Characterization* (Hansa, Munich, 1994).
32. J.H. Lee, J.W. Park, and H.B. Lee, *Biomaterials* **12** (1991) p. 443.
33. J.C. McDonald and G.M. Whitesides, *Acc. Chem. Res.* **35** (2002) p. 491. □

Coming Soon!

The New
2006 MRS Publications Catalog



Contact MRS and request
a copy today!

info@mrs.org or 724-779-3003

Advertisers in This Issue

	Page No.
Carl Zeiss MicroImaging, Inc.	149
Gatan, Inc.	81
Harrick Plasma	99
High Voltage Engineering	Inside front cover
Huntington Mechanical Labs, Inc.	Outside back cover
Janis Research Co., Inc.	128
Kurt J. Lesker Co.	Inside back cover
MMR Technologies, Inc.	99
Nanolnk, Inc.	125
Shiva Technologies, Inc.	94

For free information about the products and services offered in this issue, check www.mrs.org/bulletin_feb06_ads